Available online at www.sciencedirect.com

ScienceDirect

Energy Procedia 125 (2017) 153–160

Energy Procedia

www.elsevier.com/locate/procedia

European Geosciences Union General Assembly 2017, EGU Division Energy, Resources & Environment, ERE

High frequency ghost cavitation – a comparison of two seismic air-gun arrays using numerical modelling

Babak Khodabandeloo[a,*], Martin Landrø[a]

[a]*Department of Geoscience and Petroleum, Norwegian University of Science and Technology (NTNU), NO-7491 Trondheim, Norway*

Abstract

Ghost cavitation is probably the mechanism behind the majority of high frequencies (above 5 kHz) generated by seismic air-gun arrays. Such high frequencies are less important in seismic reflection imaging. High frequency sound might impact marine fauna and particularly marine mammals. In this paper the array signatures and high frequency ghost cavitation signals for two different arrays are simulated using numerical modelling. It is observed that one array has slightly more (20%) energy within the seismic frequency band (1-100 Hz) but emits significantly more energy (150%) for frequencies above 5 kHz.

Peer-review under responsibility of the scientific committee of the European Geosciences Union (EGU) General Assembly 2017 – Division Energy, Resources and the Environment (ERE).

Keywords: air-gun array; high frequency generation; ghost cavitation; numerical simulation

1. Introduction

Underwater ocean noise generated by human activities has increased over the last century. Seismic surveys besides shipping, military activities, and pile driving, are one of the major man-made underwater acoustic noise sources [1]. Cetaceans use acoustic waves for several essential purposes including finding prey, mating, social interaction, and avoiding predators [2]. There are widespread and increasing concerns regarding the adverse impacts of anthropogenic underwater acoustics on marine mammals which include physical and physiological effects,

* Corresponding author. Tel.: +47-73 59 46 52
E-mail address: babak.khodabandeloo@ntnu.no

1876-6102
Peer-review under responsibility of the scientific committee of the European Geosciences Union (EGU) General Assembly 2017 – Division Energy, Resources and the Environment (ERE).
10.1016/j.egypro.2017.08.158

acoustic masking, behavioral reactions, and chronic stress effects [3-5]. There are evidences of both short–and long–term behavioral changes as a result of elevated background noise. Measurements indicate that right whale calls have shifted to higher frequencies within around three decades [6] which is related to the increased noise in the frequency band of their calls. Other measurements have shown a correlation between the amount of stress hormones in whales and underwater noise [7]. Behavioral disturbances were observed in different marine mammals subjected to the noise from seismic air-guns, and it was more pronounced in smaller species [8]. During and after the end of exposure to naval sonar signal, the feeding behavior of humpback whales was interrupted [9]. As a result of operating seismic survey there was observed both increase and decrease in fish catch rates [10]. The increase in catch rate is attributed to the elevated swimming activities that can be an indicator of increase stress due to seismic shooting which in the long run may result in reduce in catch rate.

To extract the information about geological structure beneath the seabed, marine seismic reflection profiling is used. In marine seismic surveys an active source is used to generate acoustic waves that propagate into the Earth. Acoustics waves reflected at interfaces between layers with different seismic velocities are recorded by hydrophones embedded within long streamers towed behind a seismic vessel or by geophones located at the seabed. Air-gun arrays, marine vibrators and water-guns are the main marine seismic sources [11-12]. Among them, however, air-gun arrays are by far the most common and efficient seismic sources [13]. Air-guns generate impulsive acoustic waves by discharging highly pressurized air into the surrounding water [14]. An air-gun array contains several (typically 12 to 48) individual air-guns. The purpose of using air-gun arrays, instead of a single air-gun, is to increase the source strength, to focus the acoustic pressure signal in the vertical direction, and to damp unwanted bubble oscillations (that occur after the primary acoustic signal) to improve the source signature [15].

Air-gun arrays generate broad-band acoustic waves from a few Hz up to tens of kHz [16-17]. Only low frequencies (< ~100 Hz) are useful for deep seismic imaging since they penetrate deeper into the Earth. Even though high frequencies (>1000 Hz) can be used to detect gas leakage from a CO_2 storage site or an oil and gas production field [18], such higher frequencies are mostly considered as waste energies and are filtered out prior to the processing step [19]. Considering hearing curves of marine mammals it can be inferred that the emitted high frequencies from air-gun arrays may have negative impact on several cetacean species, as for instance toothed whales [17,20].

There are several underlying mechanisms for high frequency generation related to air-gun arrays. To reduce the high frequencies attributed to steep rise time of pressure waves of each individual air-gun a new air-gun has been designed and tested [21,22]. Interaction between reflected ghost wave and air-gun bubble also generates frequencies between 400 and 600 Hz [23,24]. In air-gun arrays, another underlying mechanism for generating frequencies up to tens of kHz is called ghost cavitation [17]. Recording the far-field signals from marine seismic air-gun arrays using broad band hydrophones it was observed that full air-gun arrays signals contain high frequency signal which appears few milliseconds after the ghost signal [25,26]. Reflected ghost signals from individual air-guns in the array "add up" and drop the absolute hydrostatic pressure to zero in some locations for a short time. In such regions cavities can grow and their subsequent collapse generates intense noise. Using numerical modelling ghost cavitation hypothesis was further validated [27]. Numerical modelling results indicate that ghost cavitation signal contains low frequencies in addition to the high frequencies [28].

In this paper the array signature and high frequency ghost cavitation signal from two air-gun array configurations are numerically simulated. The array configurations are compared with regard to their useful seismic frequency band and the undesired waste high frequencies generated by ghost cavitation phenomena. It is shown that selection and arrangement of individual air-guns in the array can be optimized to reduce the waste high frequencies without compromising the low frequencies that benefits seismic imaging.

Nomenclature

R	time dependent radius of cavity (m)
t	time (s)
P	external pressure (Pa)
P_i	pressure inside the cavity (Pa)

ρ	water density (kg/m^3)
c	water sound speed (m/s)
σ	water surface tension (N/m)
μ	dynamic viscosity of water (N.s/m^2)
$s_i(f)$	frequency domain representation of the time signal from the collapse of *i*th cavity
γ	absorption (Neper/m)
f	frequency (Hz)
r	distance between cavity and propagation location (m)
u_i	time signal from the collapse of *i*th cavity
y	ghost cavitation signal
N	number of cavities
E	energy of signal

2. Ghost cavitation signal modelling

An air-gun array includes several individual air-guns usually with different air chamber sizes. A full array has usually two to three sub-arrays. Acoustic pressure signal from a single air-gun modelled by the NUCLEUS^{TM} source modelling package (Petroleum Geo-Services) is shown in Fig. 1. The first peak is the direct arrival primary pulse and the other peaks are formed due to the air bubble oscillations. In an air-gun array the notional source signature from each air-gun is influenced by the acoustic pressure of the other air-guns as well.

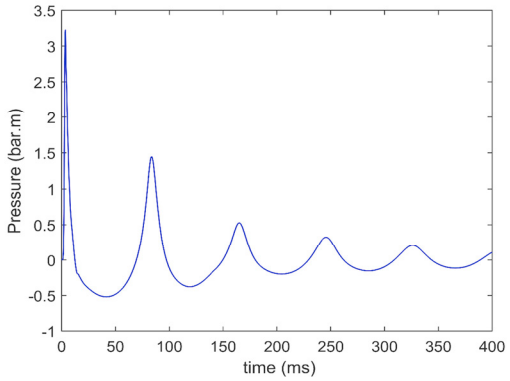

Fig. 1. Notional source signature of an individual air-gun simulated by NUCLESU^{TM} (PGS).

Numerical modelling of the ghost cavitation signal from an air-gun array is explained in [24] and can be summarized in four steps:

- *Step 1:* Spatial and temporal distributions of regions where the pressure drops below certain threshold level. Air-gun modelling is used to find the emitted acoustic pressure from each individual air-gun in the array.

- *Step 2:* Using bubble dynamics equations [29], the cavity growth and its subsequent collapse due to sudden pressure drop is estimated:

$$\left(1-\frac{1}{c}\frac{dR}{dt}\right)R\frac{d^2R}{dt^2}+\frac{4\mu}{\rho c}\frac{d^2R}{dt^2}=-\frac{3}{2}\left(1-\frac{1}{3c}\frac{dR}{dt}\right)\left(\frac{dR}{dt}\right)^2-\frac{1}{\rho R}\left(2\sigma+4\mu\frac{dR}{dt}\right)+\frac{1}{\rho}\left(1+\frac{1}{c}\frac{dR}{dt}\right)\left(P_i(t)-P\right)+\frac{R}{\rho c}\frac{dP_i(t)}{dt}. \tag{1}$$

The emitted acoustic pressure due to cavity growth and collapse at the far-field at the distance r from the cavity is estimated by the following equation [30,31]:

$$p(t)=\frac{\rho}{4\pi r}\frac{d^2V}{dt^2}=\frac{\rho R}{r}\left(2\dot{R}^2+R\ddot{R}\right) \tag{2}$$

In the above equation the superposed dot indicates a time derivative.

- *Step 3:* Each individual cavity signature is propagated to the receiver location. Geometrical spreading and absorption are included, as follows:

$$u_i(t,r)=\frac{1}{\sqrt{2\pi}}\int_{-\infty}^{+\infty}\left(s_i(f)\cdot e^{-\gamma(f)r_i}\cdot e^{-j2\pi f\tau_i}\cdot\frac{e^{-j\frac{2\pi f}{c}r_i}}{r_i}\right)\cdot e^{j2\pi ft}df \tag{3}$$

- *Step 4:* The ghost cavitation signal is formed by adding acoustic signatures from individual cavities:

$$y(t,r)=\sum_{i=1}^{N}u_i \tag{4}$$

3. Two air-gun arrays configurations

The configuration of two different air-gun arrays is shown in Fig. 2. Both arrays consist of three sub-arrays. The first air-gun array is shown in Fig. 2 (a) and hereafter is called array 1.

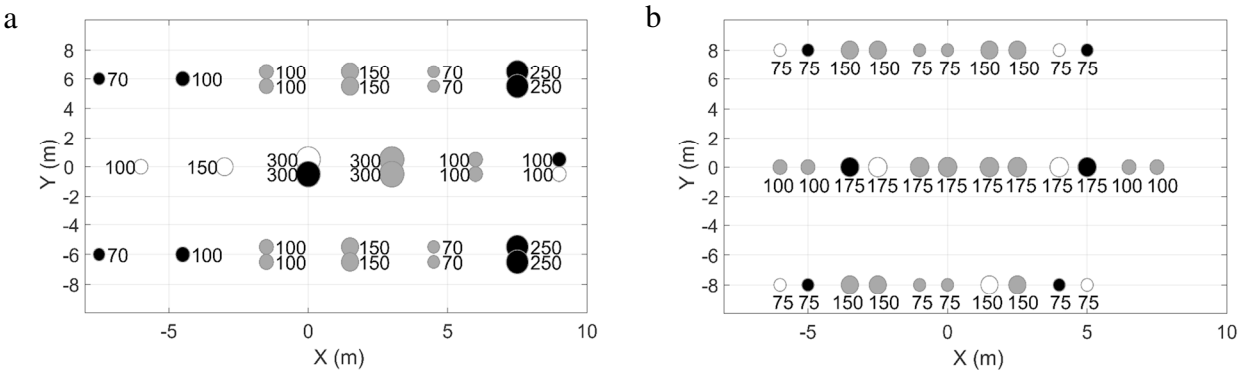

Fig. 2. Two air-gun array configurations. Circles indicate individual air-guns in the array and the numbers show the air chamber volume of each air-gun. White, gray, and black colors indicate single air-gun, cluster, and inactive air-guns, respectively. (a) Array 1, with 6 meters subarray separation and total volume of 2730 in^3; (b) Array 2, with 8 meters subarray separation and total volume of 3250 in^3.

The distance between the sub-arrays is 6 meters for array 1, and the corresponding separation distance is 8 meters for array 2. The volume of active air-guns for array 1 is 2730 in^3 and 3250 in^3 for array 2.

4. Results

For the two array configurations the regions around each array that the pressure drops below the selected threshold pressure (-0.1 bar) are numerically simulated (step 1 in section 2). The results are plotted at four time instants in Fig. 3 and Fig. 4 for array 1 and 2, respectively. In the second row of the figures the cut sections of the regions are plotted and it is observed that array 2 has stronger negative pressures than array 1.

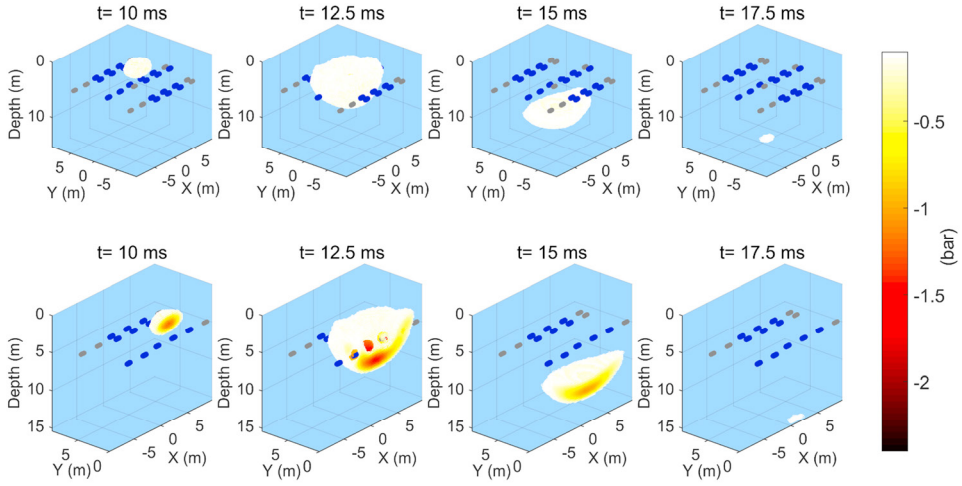

Fig. 3. Top row: regions where the absolute hydrostatic pressure drops the threshold pressure (-0.1 Bar) at four time instants for array 1. The active air-guns and inactive ones in the array are shown by blue and gray, respectively. Bottom row: cut sections of images shown in the top row.

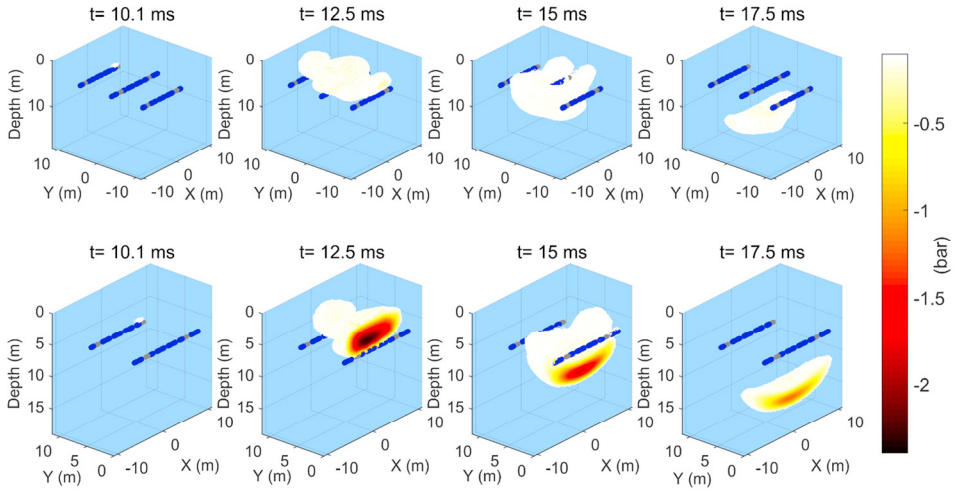

Fig. 4. Top row: regions where the absolute hydrostatic pressure drops the threshold pressure (-0.1 Bar) at four time instants for array 2. The active air-guns and inactive ones in the array are shown by blue and gray, respectively. Bottom row: cut sections of images shown in the top row.

Thereafter, for both of the array configurations, the array signatures (including the ghost cavitation signal) are plotted in Fig. 5(a). These signals are simulated for a location 55 meters vertically below each array and with 40 meters offset. In Fig. 5(b), 5 kHz high passed (HP) filtered signals are plotted for array 1 and 2. Such high frequencies are generated by the ghost cavitation phenomena. It is seen that the maximum amplitude of the HP filtered signal for array 2 is almost 2.5 times more compared to array 1.

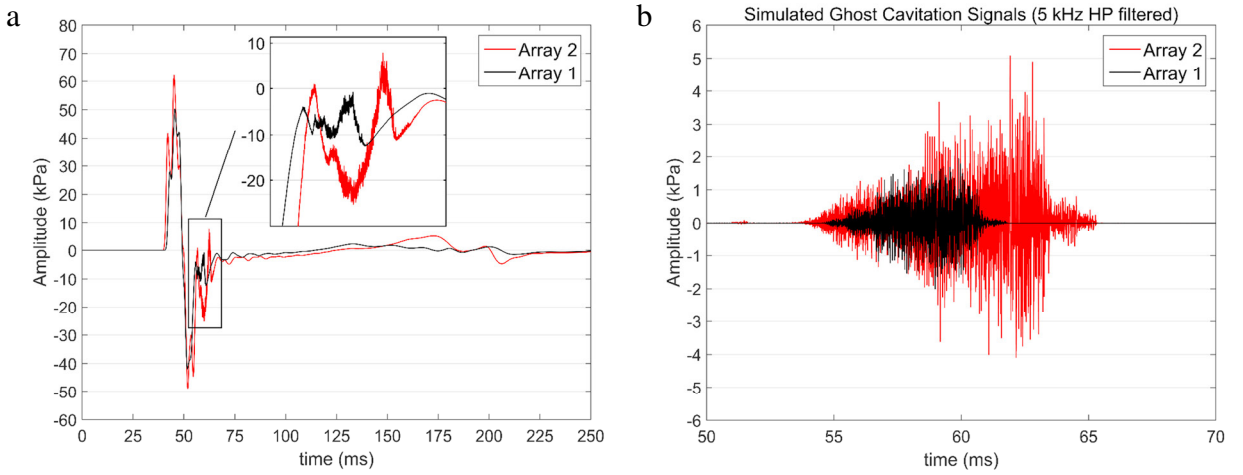

Fig. 5. (a) Computed array signatures for array configurations 1 and 2. No filter applied; (b) 5 kHz HP filtered signals for the same signals shown in (a). Notice the stronger and longer ghost cavitation signal for array 2.

Energy spectrums of both signals shown in Fig. 5(a) are plotted in Fig 6. It is clear that array 2 generates more high frequencies (>5 kHz) while it has only slightly higher energy level in the seismic frequency range. The energy level of array 2 is around 10 dB higher than array 1 in almost the whole frequency range between 5-70 kHz.

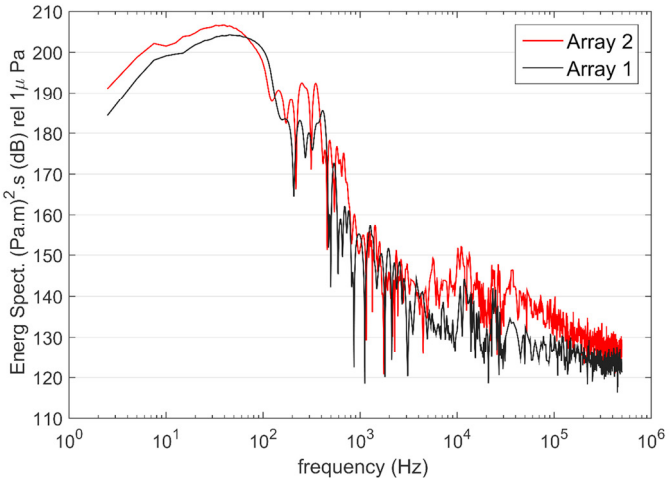

Fig. 6. Energy spectrum of simulated signals for array 1 and array 2 shown in Fig. 5(a). Above 3 kHz the graphs are smoothed.

Energies of the signals at different frequency bands for both arrays are compared in Fig. 7. The energies are used instead of RMS values since for transient signals the RMS will be influenced by the selected time duration. The energy is defined as:

$$E = \sqrt{dt \times \sum_{i=1}^{N} x_i^2} \tag{5}$$

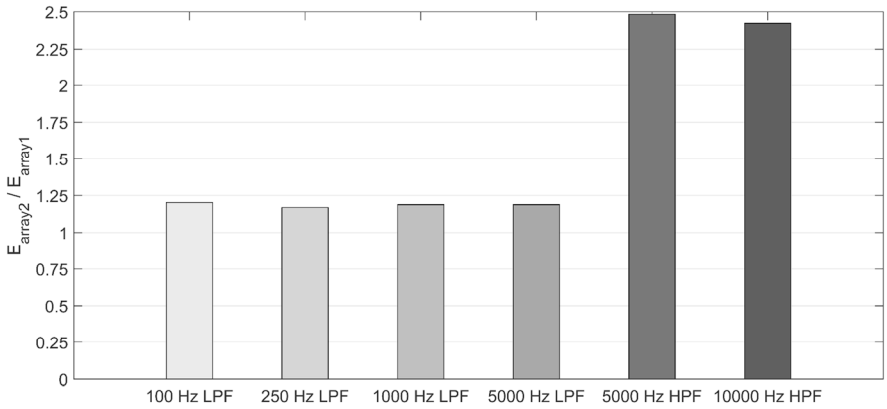

Fig. 7. Ratio of energy levels for array 1 and 2 at different frequency ranges. (LPF: Low Passed Filtered; HPF: High Passed Filtered).

In Fig. 7 the energy of both arrays are compared at different frequency ranges. It is observed that the energy of array 2 at low frequencies (<100 Hz) which benefits the deep seismic imaging is around 20% more than the useful energy of array 1. But, array 2 generates around 148% more high frequencies (>5 kHz) compared the array 1. Such high frequencies are less important for seismic imaging and might impact marine life.

5. Discussion and conclusions

Numerical simulation is used to simulate the high frequency ghost cavitation signal as well as the source signature for two different seismic air-gun arrays. Both arrays have three sub-arrays and in one of them the sub-arrays are separated by 6 meters while in the other one the separation distance is 8 meters. Total air chamber volumes for the two arrays are 2730 in^3 and 3250 in^3, respectively. Even though the sub-array distance in the larger array is more, the air-guns in each of its sub-array are located closer to each other and have more uniform distributions. It is observed that both the peak amplitude and beneficial low frequency (<100 Hz) energy content of the larger array for deep seismic imaging is approximately 20% more than the smaller array. However, it emits around 150% more high frequency (> 5 kHz) energy. The duration of the high frequency signal for array 2 is around twice as much compared to array 1. Hence, the smaller array configuration is regarded to be more environmental friendly. We suggest that numerical simulation can be used to select and arrange air-gun arrays in order to reduce the amount of unwanted high-frequency signals.

Acknowledgements

This research is funded by Research Center for Arctic Petroleum Exploration (ARCEx) partners, and the Research Council of Norway (Grant No. 228107). Statoil grant for publication is also gratefully acknowledged.

References

[1] Hildebrand, John A. "Anthropogenic and natural sources of ambient noise in the ocean." *Marine Ecology Progress Series* 395 (2009): 5-20 (doi:10.3354/meps08353)

[2] Wright, Andrew J., Natacha Aguilar Soto, Ann Linda Baldwin, Melissa Bateson, Colin M. Beale, Charlotte Clark, Terrence Deak et al. "Do marine mammals experience stress related to anthropogenic noise?" International Journal of Comparative Psychology 20, no. 2 (2007).

[3] Richardson, W. J., Greene, C. R., Jr., Malme, C. I., and Thomson, D. H. (1995). Marine Mammals and Noise (Academic Press, New York), Chap. 1.
[4] National Research Council 2003 Ocean noise and marine mammals. Washington, DC: National Academies Press.
[5] Gordon, Jonathan, Douglas Gillespie, John Potter, Alexandros Frantzis, Mark P. Simmonds, René Swift, and David Thompson. "A review of the effects of seismic surveys on marine mammals." *Marine Technology Society Journal* 37, no. 4 (2003): 16-34.
[6] Parks, Susan E., Christopher W. Clark, and Peter L. Tyack. "Short-and long-term changes in right whale calling behavior: the potential effects of noise on acoustic communication." *The Journal of the Acoustical Society of America* 122, no. 6 (2007): 3725-3731.
[7] Rolland, Rosalind M., Susan E. Parks, Kathleen E. Hunt, Manuel Castellote, Peter J. Corkeron, Douglas P. Nowacek, Samuel K. Wasser, and Scott D. Kraus. "Evidence that ship noise increases stress in right whales." *Proceedings of the Royal Society of London B: Biological Sciences* 279, no. 1737 (2012): 2363-2368.
[8] Stone, Carolyn J., and Mark L. Tasker. "The effects of seismic airguns on cetaceans in UK waters." *Journal of Cetacean Research and Management* 8, no. 3 (2006): 255.
[9] Sivle, Lise Doksæter, Paul J. Wensveen, Petter H. Kvadsheim, Frans-Peter A. Lam, Fleur Visser, Charlotte Curé, Catriona M. Harris, Peter L. Tyack, and Patrick JO Miller. "Naval sonar disrupts foraging in humpback whales." Marine Ecology Progress Series 562 (2016): 211-220.
[10] Løkkeborg, S., E. Ona, A. Vold, H. Pena, A. Salthaug, B. Totland, J. T. Øvredal, J. Dalen, and N. O. Handegard, *Effects of seismic surveys on fish distribution and catch rates of gillnets and longlines in Vesterålen in summer 2009*. Fisken og Havet No 2, The Institute of Marine Research (2010).
[11] Duren, Richard E. "A theory for marine source arrays." *Geophysics* 53, no. 5 (1988): 650-658.
[12] Barger, James E., and William R. Hamblen. "The air gun impulsive underwater transducer." *The Journal of the Acoustical Society of* America 68, no. 4 (1980): 1038-1045.
[13] Watson, Leighton, Eric Dunham, and Shuki Ronen. "Numerical modeling of seismic airguns and low-pressure sources." In *SEG Technical Program Expanded Abstracts* 2016, pp. 219-224. Society of Exploration Geophysicists, 2016.
[14] Caldwell, Jack, and William Dragoset. "A brief overview of seismic air-gun arrays." *The leading edge* 19, no. 8 (2000): 898-902.
[15] Dragoset, Bill. "Introduction to air guns and air-gun arrays." *The Leading Edge* 19, no. 8 (2000): 892-897.
[16] Goold, John C., and Peter J. Fish. "Broadband spectra of seismic survey air-gun emissions, with reference to dolphin auditory thresholds." *The Journal of the Acoustical Society of America* 103, no. 4 (1998): 2177-2184.
[17] Landrø, M., L. Amundsen, and D. Barker. "High-frequency signals from air-gun arrays." *Geophysics* 76, no. 4 (2011): Q19-Q27.
[18] Landrø, Martin, Fredrik Hansteen, and Lasse Amundsen. "Detecting gas leakage using high-frequency signals generated by air-gun arrays." *Geophysics* 82, no. 2 (2017): A7-A12.
[19] Ronen, Shuki, Stuart Denny, Rob Telling, Steve Chelminski, John Young, Don Darling, and Seibert Murphy. "Reducing ocean noise in offshore seismic surveys using low-pressure sources and swarms of motorized unmanned surface vessels." In *SEG Technical Program Expanded Abstracts* 2015, pp. 4956-4960. Society of Exploration Geophysicists, 2015.
[20] Ketten, Darlene R. "Marine mammal auditory systems: a summary of audiometric and anatomical data and implications for underwater acoustic impacts." *Polarforschung* 72, no. 2/3 (2004): 79-92.
[21] Coste, Emmanuel, David Gerez, Halvor Groenaas, Jon-Fredrik Hopperstad, Ola Pramm Larsen, Robert Laws, Jack Norton, Matthew Padula, and Michel Wolfstirn. "Attenuated high-frequency emission from a new design of air-gun." In *84th Annual International Meeting, SEG, Expanded Abstracts*, pp. 132-137. 2014.
[22] Gerez, David, Halvor Groenaas, Ola Pramm Larsen, Michel Wolfstirn, and Matthew Padula. "Controlling air-gun output to optimize seismic content while reducing unnecessary high-frequency emissions." In *SEG Technical Program Expanded Abstracts* 2015, pp. 154-158. Society of Exploration Geophysicists, 2015.
[23] King, J. R. C., A. M. Ziolkowski, and M. Ruffert. "Boundary conditions for simulations of oscillating bubbles using the non-linear acoustic approximation." *Journal of Computational Physics* 284 (2015): 273-290.
[24] King, Jack RC. "Air-gun bubble-ghost interactions." *Geophysics* 80, no. 6 (2015): T223-T234.
[25] Landrø, Martin, Lasse Amundsen, and Jan Langhammer. "Repeatability issues of high-frequency signals emitted by air-gun arrays." *Geophysics* 78, no. 6 (2013): P19-P27.
[26] Landrø, Martin, Yuan Ni, and Lasse Amundsen. "Reducing high-frequency ghost cavitation signals from marine air-gun arrays." *Geophysics* 81, no. 3 (2016): P33-P46.
[27] Khodabandeloo, Babak, Martin Landrø, and Alfred Hanssen. "Acoustic generation of underwater cavities—Comparing modeled and measured acoustic signals generated by seismic air gun arrays." *The Journal of the Acoustical Society of America* 141, no. 4 (2017): 2661-2672.
[28] Khodabandeloo, Babak. and Martin Landrø, "Effects of ghost cavitation cloud on near-field hydrophones measurements in the seismic airgun arrays". In *79th EAGE Conference and Exhibition-Workshops* 2017 Paris 12 – 15 June, Paper Tu A4 09.
[29] Prosperetti, A., and A. Lezzi. "Bubble dynamics in a compressible liquid. Part 1. First-order theory." *Journal of Fluid Mechanics* 168 (1986): 457-478.
[30] Brennen, Christopher E. (2013). Cavitation and Bubble Dynamics (Cambridge University Press, London).
[31] Leighton, Timothy. (2012). The Acoustic Bubble (Academic Press, New York).